New Synthetic and Structural Aspects in the Chemistry of Alkylaluminum Fluorides. The Mutual Influence of Hard and Soft Ligands and the Hybridization as Rigorous Structural Criterion[#]

Marilena Ferbinteanu,[†,‡] Herbert W. Roesky,*[,†] Fanica Cimpoesu,[§] Mihail Atanasov,[∥,⊥] Sinje Köpke,[†] and Regine Herbst-Irmer[†]

Institut für Anorganische Chemie der Universität Göttingen, Tammannstrasse 4, D-37077 Göttingen, Germany, Institute of Physical Chemistry, Splaiul Independentei 202, 77208 Bucharest, Romania, and Institut für Theoretische Chemie der Heinrich-Heine Universität, Universitätsstrasse 1, D-40225 Düsseldorf, Germany

Received January 31, 2001

A general synthetic strategy starting from metal alkyls is reported based on the hydrogen difluoride anion as a suitable reagent for obtaining organometallic fluorides. The newly prepared compounds are $[Me_4N][(i\text{-}Bu)_2AlF_2]$ (**1**), $[Ph_4P][(i\text{-}Bu)_2AlF_2]$ (**2**), and $[Ph_4P][AlF_4]$ (**3**), containing the tetrahedral anions $[(i\text{-}Bu)_2AlF_2]^-$ and $[AlF_4]^-$. The actual structures are prototypes that allowed a comparison of inorganic and organometallic fluorides in the frame of the *hard and soft acid and base* principle, by means of ab initio calculations. A new theoretical model is designed to put in equation form the qualitative statements of the Bent rule. The model allows the rationalization of the tendencies of bond angle variation in $[R_2MX_2]$ systems containing a main group metal (M), in terms of hybridization of the central atom and the reciprocal influence of hard and soft ligands.

Introduction

Following our general interest in organometallic fluorides,[1,2] the compounds reported herein are prototypes for the correlation of inner structural features with the idea of hybridization and including the *hard and soft acid and base principle* (HSAB).[3] This work compares the organometallic fluorides $[Me_4N][(i\text{-}Bu)_2AlF_2]$ (**1**) and $[Ph_4P][(i\text{-}Bu)_2AlF_2]$ (**2**) with the inorganic anion of $[Ph_4P][AlF_4]$ (**3**) as a model.

Compound **3** is in line with the HSAB principle, containing aluminum as a hard acid and fluorine as a hard base. The chemical hardness,[4] a quantitative measure of Lewis basicity or acidity, approximately parallels the electronegativity,[5] and in this view, fluorine and alkyl groups as ligands appear to be rather different. Consequently, the organometallic fluorides **1** and **2** are not in agreement with the HSAB principle, but this does not preclude their formation. Moreover, the properties of hard (F) and soft (R) ligands in $[R_2AlF_2]^-$ are averaged at the expense of each other (see mutual influence).

The interest in organoaluminum fluorides stems from the potential importance[6] of these compounds as models for certain catalytic reactions. Thus, organoaluminum fluorides can be found among the pioneering work of Ziegler.[7] The well-known MAO (methylalumoxane) cocatalyst[8] seems to have, analogously to organometallic fluorides, a structure based on methyl and oxygen ligands with different HSAB characteristics. Inorganic fluorides and oxo-fluorides prepared from $[AlF_4]^-$ sources function also as catalysts.[9,10]

Therefore we are interested in understanding the bonding of the $[R_2AlF_2]^-$ and $[AlF_4]^-$ anions in terms of HSAB factors as a useful addition to the known correlations between HSAB parameters and catalytic activity.[11]

A general strategy for the synthesis of compounds with hard and soft ligands is the use of reagents containing the hydrogen

[#] Dedicated to Professor Hans Bürger on the occasion of his 65th birthday.

[†] Institut für Anorganische Chemie der Universität Göttingen.

[‡] Permanent address: University of Bucharest, Faculty of Chemistry, Inorganic Chemistry Department, Dumbrava Rosie 23, Bucharest 70254, Romania. E-mail: mcimpoesu@yahoo.com.

[§] Institute of Physical Chemistry, Bucharest.

[∥] Institut für Theoretische Chemie der Heinrich-Heine Universität.

[⊥] On leave of absence from the Institute of General and Inorganic Chemistry, Bulgarian Academy of Science, Sofia, Bulgaria.

(1) (a) Witt, M.; Roesky, H. W. *Prog. Inorg. Chem.* **1992**, *40*, 353−444. (b) Liu, F.-Q.; Usón, I.; Roesky, H. W. *J. Chem. Soc.* **1995**, 2453−2458. (c) Murphy, E. F.; Lübben, T.; Herzog, A.; Roesky, H. W.; Demsar, A.; Noltemeyer, M.; Schmidt, H.-G. *Inorg. Chem.* **1996**, *35*, 23−29. (d) Roesky, H. W.; Herzog, A.; Liu, F.-Q. *J. Fluorine Chem.* **1995**, *71*, 161−161. (e) Roesky, H. W. *Inorg. Chem*. **1999**, *38*, 5934−5943.

(2) Jagirdar, B. R.; Murphy, E. F.; Roesky, H. W. *Prog. Inorg. Chem.* **1999**, *48*, 351−455.

(3) (a) Pearson, R. G. *J. Am. Chem. Soc.* **1963**, *85*, 3533−3539. (b) Pearson R. G. *Inorg. Chem.* **1988**, *27*, 734−740. (c) Archland, S. *Coord. Chem. Rev.* **1996**, *154*, 13−18.

(4) Pearson R. G. *Struct. Bond.* **1993**, *80*, 1−11.

(5) Pearson, R. G. In *Theoretical Model of Chemical Bonding*; Maksic, Z. B., Ed.; Springer-Verlag: Berlin, 1990.

(6) Atwood, D. A.; Yaerwood, B. C. *J. Organomet. Chem.* **2000**, *600*, 186−197.

(7) Ziegler, K.; Köster, R. *Liebigs Ann. Chem*. **1957**, *608*, 1−7.

(8) Fink, G., Mülhaupt, R., Brintzinger, H. H., Eds. *Ziegler Catalysts: Recent Scientific Innovations and Technological Improvements*; Springer-Verlag: Berlin, 1995.

(9) (a) Kemnitz, E.; Menz, D. H. *Prog. Solid Chem.* **1998**, *26*, 97−153. (b) Herron, N.; Farneth, W. E. *Adv. Mater.* **1996**, *8*, 959−963. (c) DeCanio, E. C.: Bruno, J. W.; Nero V. P.; Edwards, J. C. *J. Catal.* **1993**, *140*, 84−89. (d) Bentrup, U. *Eur. J. Solid State Inorg. Chem.* **1992**, *29*, 51−54.

(10) Timoshkin, A. Y.; Suvorov, A. V.; Bettinger, H. F.; Schaefer, H. F. *J. Am. Chem. Soc*. **1999**, *121*, 5687−5699.

(11) (a) Mortier, W. J., Moffat, J. B., Eds. *Theoretical Aspects of Heterogeneous Catalysis*; Van Nostrand Reinhold: New York, 1990. (b) Mortier, S. K.; Ghoshi, S.; Shankar, S. *J. Am. Chem. Soc.* **1986**, *108*, 4315−4320. (c) Louwen, J. N.; Voght, E. T. C. *J. Mol. Catal. A, Chem.* **1998**, *134*, 63−77. (d) Rappe, A. K.; Goddard, W. A. *J. Phys. Chem*. **1991**, *95*, 3358−3363. (e) Boekelandt, B. G.; Mortier W. J.; Schoenheydt, R. A. *Struct. Bond*. **1993**, *80*, 189−226.

10.1021/ic010131g CCC: $20.00
Published on Web 08/07/2001

difluoride anion $[FHF]^-$ and its reaction with metal alkyls. The $[FHF]^-$ anion is a species with remarkable properties[12−14] and can be regarded as the simplest coordination compound containing the smallest positive ion (proton). The reaction of $[FHF]^-$ with MR_n leads to the organometallic fluoride ($MR_{n-x}F_x$) under evolution of alkane (RH). This process is not of HSAB type. Indeed, the hardest acid (H^+) approaches the weakest Lewis base of the system (R^-), and vice-versa, the hardest base (F^-) leaves its hard partner. The proton from $[FHF]^-$ helps to override[15] the usual HSAB direction of a reaction, leading to organometallic fluorides by a rational route.

The $[FHF]^-$ formed in situ can be found as a bridging block between two metal centers.[16−18] The number of such compounds can be increased when the anion is directly introduced as an ammonium salt.

Experimental Section

General Procedures. All experiments were performed using standard Schlenk techniques under a dry nitrogen atmosphere due to the extreme sensitivity of the reactants toward air and moisture. A Braun Labmaster 130 drybox was used to store the compounds and to prepare the samples for spectroscopic characterizations. Purification and drying of the solvents were done by standard methods.[19] Triisobutylaluminum (Witco) was used as received; $[Me_4N]HF_2$ and $[Ph_4P]HF_2$ were prepared as described in the literature.[20,21] The ^{1}H, ^{13}C, and ^{19}F NMR spectra were recorded on Bruker AM 200 and Bruker AM 250 spectrometers. The standards were TMS (external; ^{1}H, ^{13}C) and C_6F_6 (external; ^{19}F) using the δ scale. FAB mass spectra were obtained on Finnigan MAT 8230 or Varian MAT CH 5 instruments, and FT-IR spectra were measured on a Bio-Rad FTS-7 as Nujol mulls between KBr plates in the range 4000−400 cm^{-1} (abbreviations used: vs, very strong; s, strong; m, medium; w, weak). Elemental analyses were performed by the Analytisches Labor des Instituts für Anorganische Chemie der Universität Göttingen. Melting points were measured with a HWS-SG 3000 apparatus in sealed capillaries under nitrogen (values not corrected).

Synthesis of $[Me_4N][(i\text{-}Bu)_2AlF_2]$ (1). A solution of Al(*i*-Bu)$_3$ (0.4 g, 2.03 mmol) in toluene was added dropwise to a suspension of $[Me_4N]HF_2$ (0.23 g, 2.03 mmol) in toluene (30 mL), and the mixture was stirred for 2 h at −30 °C. After heating slowly, the resulting solution was filtered, and the filtrate was kept at room temperature. Colorless crystals of **1** could be isolated (0.47 g, 93%) after 2 weeks. Mp: 81 °C. ^{1}H NMR (200 MHz, C_6D_6, ppm): δ −0.42 (d, 4H, ^3J(HH) = 6.5 Hz, Al−C*H*$_2$CH(CH$_3$)$_2$), 0.86 (d, 12H, ^3J(HH) = 6.5 Hz, Al−CH$_2$CH(C*H*$_3$)$_2$), 1.6 (m, 2H, Al−CH$_2$C*H*(CH$_3$)$_2$), 2.42 (s, 12H, *CH*$_3$). ^{13}C NMR (126 MHz, C_6D_6, TMS, ppm): δ 28.5 (Al−*C*H$_2$CH(CH$_3$)$_2$), 29.2 (Al−CH$_2$CH(*C*H$_3$)$_2$), 30.1 (Al−CH$_2$*C*H(CH$_3$)$_2$) (analogously to data reported in ref 22), 55.1 ((*C*H$_3$)$_4$N$^+$). ^{19}F NMR (188 MHz, C_6D_6, C_6F_6, ppm): δ 12.60 ($\Delta\nu_{1/2}$ = 180 Hz). IR (cm^{-1}): 663 (s) (ν Al−F) (comparable with data from ref 23), 695 (m), 724 (m) (ν Al−F) (comparable with data from ref 36), 803 (s), 863 (m), 911 (m), 949 (m), 1036 (s), 1096 (s), 1262 (s), 1602 (m), 1626 (m), 1725 (w). MS (EI): *m*/*z* (%): 74 (100, Me_4N^+), 57 (10, $(C_4H_9)^+$). Negative ion FAB-MS (3-NBA matrix):[24] *m*/*z* 179 ([(*i*-Bu)$_2$AlF$_2$]). Anal. Calcd for $C_{12}H_{30}AlF_2N$ (M_r 253.35): C, 56.91; H, 11.85; Al, 10.67. Found: C, 56.8; H, 10.4; Al, 10.5.

Synthesis of $[Ph_4P][(i\text{-}Bu)_2AlF_2]$ (2). A solution of Al(*i* -Bu)$_3$ (1.05 g, 5.3 mmol) in toluene was added dropwise to a suspension of $[Ph_4P]HF_2$ (2 g, 5.3 mmol) in toluene (40 mL). The synthesis conditions for **2** are similar to those for **1**. A colorless powder was isolated after 2 days (2.7 g, 89.8%) and decomposes slowly > 140 °C. ^{1}H NMR (200 MHz, CD_3CN, ppm): δ −0.4 (d, 4H, ^3J(HH) = 5.2 Hz, Al−C*H*$_2$CH(CH$_3$)$_2$), 0.89 (d, 12H, Al−CH$_2$CH(*CH*$_3$)$_2$), 1.6 (m, 2H, Al−CH$_2$*CH*(CH$_3$)$_2$), 7.64, 7.87 (m, 20H, [(C$_6$*H*$_5$)$_4$P]$^+$). ^{13}C NMR (126 MHz, CD_3CN, TMS, ppm): δ 28.5 (Al−*C*H$_2$CH(CH$_3$)$_2$), 29.2 (Al−CH$_2$CH(*C*H$_3$)$_2$), 30.1 (Al−CH$_2$*C*H(CH$_3$)$_2$),[22] 118.5, 119.3, 131.2, 135.7, 136.4 [(*C*$_6$H$_5$)$_4$P]$^+$). ^{19}F NMR (188 MHz, C_6D_6, C_6F_6, ppm): δ 10.3. IR (cm^{-1}): 527 (s), 650 (m) (ν Al−F),[23] 690 (s), 723(m) (ν Al−F),[36] 753-(s), 787 (s), 853 (w), 996 (m), 1108 (s), 1169, 1187 (w), 1315 (m), 1585 (m). MS (EI): *m*/*z* (%): 339 (100, [(C$_6$*H*$_5$)$_4$P]$^+$). Negative ion FAB-MS (3-NBA matrix):[24] *m*/*z* 179 ([(*i*-Bu)$_2$AlF$_2$]$^-$). Anal. Calcd for $C_{32}H_{38}AlF_2P$ (M_r 518.57): C, 74.13; H, 7.33; Al, 5.21; P, 5.98. Found: C, 73.8; H, 7.3; Al, 5.3; P, 6.1.

Synthesis of $[Ph_4P][AlF_4]$ (3). A solution of $[Ph_4P]HF_2$ (0.45 g, 1.2 mmol, excess) in THF (10 mL) was added slowly to a suspension of $[Ph_4P][(i\text{-}Bu)_2AlF_2]$ (0.31 g, 0.6 mmol) in toluene (30 mL). The mixture was stirred for 2 h at 80 °C, and after cooling, the resulting solution was filtered, and the filtrate kept at room temperature. Colorless crystals of **3** were isolated after 3 days (2.3 g, 87%). Mp: 348 °C. ^{1}H NMR (500 MHz, CD_3CN, ppm): δ 7.67, 7.72, 7.90 (m, 20H, ^3J(HH) = 5.2 Hz, [(C$_6$*H*$_5$)$_4$P]$^+$). ^{13}C NMR (126 MHz, CD_3CN, TMS, ppm): δ 118.5, 119.3, 131.2, 135.7, 136.4 [(*C*$_6$H$_5$)$_4$P]$^+$). ^{19}F NMR (188 MHz, CD_3CN, C_6F_6, ppm): δ −30.04 (sextet, I(^{27}Al) = 5/2, $^1J_{F-Al}$ = 37.5 Hz). The sextet of approximately equal intensities is a characteristic of isolated $[AlF_4]^-$ tetrahedra in solution.[25] IR (cm^{-1}): 303 (s), 447 (w), 527 (s), 616 (w), 630 (s), 724, 752 (m), 783 (s), 853 (w), 996 (m), 1026 (w), 1108 (s), 1163 (w), 1316 (w), 1436 (s), 1483 (m), 1586 (m), 1683 (w). The IR band at 783 is characteristic of the $[AlF_4]^-$ anion in

(12) Tuck, D. G. *Prog. Inorg. Chem.* **1968**, *9*, 161−194.
(13) (a) Harmon, K. M.; Alderman, S. D.; Benker, K. E.; Diestler, D. J.; Gebauer, P. A. *J. Am. Chem. Soc*. **1965**, *87*, 1700−1706. (b) Gennick, I.; Harmon, K. M.; Potvin, M. *Inorg. Chem*. **1977**, *16*, 2033−2040.
(14) (a) Silva, M. R.; Paixao, J. A.; Beja, A. M. *Acta Crystallogr. C* **2000**, *56*, 104−106. (b) Kruh, R.; Fuwa, K.; McEver, T. E. *J. Am. Chem. Soc*. **1956**, *78*, 4256−4258.
(15) HSAB principles concern general stability rules for electronic structures, but the proton possesses no electron and can be considered out of the proper model. At the same time, while the HSAB affinities are confined with rather weak interactions, the strong polarization exerted by the proton is at a higher energy compared to the normal range of the HSAB scheme.
(16) (a) Roesky, H. W.; Sotoodeh, M.; Xu, Y. M.; Schrumpf, F.; Noltemeyer, M. *Z. Anorg. Allg. Chem*. **1990**, *580*, 131−138. (b) Bentrup, U.; Harms, K.; Massa, W.; Pebler, J. *Solid State Sci*. **2000**, *2*, 373−376.
(17) (a) Jasim, N. A.; Perutz, R. N. *J. Am. Chem. Soc*. **2000**, *122*, 8685−8693. (b) Richmond, T. G. *Coord. Chem. Rev*. **1990**, *105*, 221−250.
(18) Roesky, H. W.; Haiduc, I. *J. Chem. Soc., Dalton Trans.* **1999**, 2249−2264.
(19) Perrin, D. D.; Armarego, W. L. F.; Perrin, D. R. *Purification of Laboratory Chemicals*, 2nd ed.; Pergamon Press: Oxford, 1980.
(20) Cousseau, J.; Albert, P. *Bull. Soc. Chim. Fr*. **1986**, *6*, 910−915.
(21) Brown, S. J.; Clark, J. H. *J. Fluorine Chem*. **1985**, *30*, 251−258.
(22) Kopp, M. R.; Kräuter, T.; Werner, B.; Neumüller, B. *Z. Anorg. Allg. Chem.* **1998**, *624*, 881−886.
(23) Neumüller, B. *Coord. Chem. Rev*. **1997**, *158*, 69−101.
(24) Compounds **1**−**3** produce some of the expected signals in the FAB (negative-ion) mass spectrum next to the signals for the matrix (3-nitrobenzyl alcohol, 3-NBA).
(25) Herron, N.; Thorn, D. L.; Harlow, R. L.; Davidson, F. J. *J. Am. Chem. Soc*. **1993**, *115*, 3028−3029.
(26) Herron, N.; Harlow, R. L.; Thorn, D. L. *Inorg. Chem.* **1993**, *32*, 2985−2986.
(27) Kottke, T.; Stalke, D. *J. Appl. Crystallogr*. **1993**, *26*, 615−619.
(28) Sheldrick, G. M. *Acta Crystallogr., Sect. A.* **1990**, *46*, 467−473.
(29) Sheldrick, G. M. *SHELX97*; University of Göttingen, 1997.
(30) The two imaginary values of frequency are obtained, for example, with 3-21G* or SV(P) bases in the RHF calculations. Other basis and methods may give real and low values for the same modes, supporting also the physical picture of a floppy skeleton.
(31) Batten, S. R.; Harris, A. R.; Murray, K. S. *Acta Crystallogr*. **2000**, *C56*, 1394−1395.
(32) (a) Murphy, V. J.; Hascall, T.; Chen, J. Y.; Parkin, G. *J. Am. Chem. Soc*. **1996**, *118*, 7428−7429. (b) Whittlesey, M. K.; Perutz, R. N.; Greener, B.; Moore, M. H. *Chem. Commun.* **1997**, 187−188.
(33) (a) Bosch, P.; Camps, F.; Chamorro, E.; Gasol, V.; Guerero, A. *Tetrahedron Lett*. **1987**, *28*, 4733−4736. (b) Clark, J. H. *Chem. Rev*. **1980**, *80*, 429−452.
(34) Cousseau, J.; Albert P. *J. Chem. Soc., Chem. Commun.* **1985**, *14*, 961−962.
(35) Landini, D.; Molinari, H.; Penso, M.; Rampoldi, A. *Synthesis* **1988**, *12*, 953−955.
(36) Roesky, H. W.; Stasch, A.; Hatop, H.; Rennekamp, C.; Hamilton, D. H.; Noltemeyer, M.; Schmidt, H. G. *Angew. Chem., Int. Ed.* **2000**, *39*, 171−173; *Angew. Chem*. **2000**, *112*, 177−179.

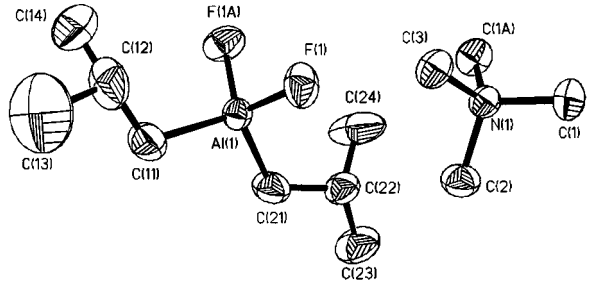

Figure 1. Molecular structure of $[Me_4N][(i\text{-}Bu)_2AlF_2]$ (**1**).

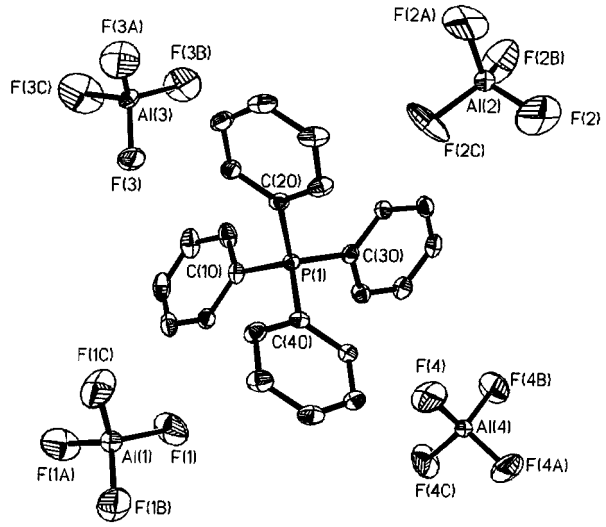

Figure 2. Molecular structure of $[Ph_4P][AlF_4]$ (**3**). Selected bonds lengths (Å) and angles (deg): Al(1)−F(1) 1.647(2), P(1)−C(10) 1.799(2), P(1)−C(20) 1.797(2), P(1)−C(30) 1.796(2), P(1)−C(40) 1.792(2); F(1)−Al(1)−F(1A) 109.9(1), F(1)−Al(1)−F(1B) 108.6(2), F(4)−Al(1)−F(4A) 110.28(8), F(4)−Al(1)−F(4B) 107.9(2), C(20)−P(1)−C(10) 110.9(1), C(30)−P(1)−C(10) 107.4(1).

solid state.[26] MS (EI): *m*/*z* 339 ($[(C_6H_5)_4P]^+$). Anal. Calcd for $C_{24}H_{20}AlF_4P$ (M_r 442.35): C, 65.22; H, 4.53; Al, 6.11. Found: C, 64.6; H, 5.0; Al, 6.3.

X-ray Structure Determination of 1 and 3. The crystals were mounted on a glass fiber with perfluoropolyether and flash-cooled to 133(2) K in a stream of nitrogen gas.[27] Diffraction data were collected on a Stoe-Siemens-Huber four-circle diffractometer coupled to a Siemens CCD area detector with graphite-monochromated Mo Kα radiation (λ = 0.71073 Å) performing φ- and ω-scans. The structure was solved by direct methods using SHELXS-97[28] and refined using F^2 on all data by full-matrix least squares with SHELXL-97.[29] All nonhydrogen atoms were refined anisotropically. Hydrogen atoms were included on calculated positions and refined using a riding model.

Crystal Structures of 1 and 3. The structures are mononuclear complexes of aluminum with a distorted tetrahedron in the case of **1** (Figure 1) and an almost regular tetrahedron for **3** (Figure 2). The cell parameters and summary of crystallographic data are compiled in Table 1. Structure **1** shows substantial disorder. Both ions of **1** lie on mirror planes, but in the anion only the $[C_2AlF_2]$ part fulfills this symmetry, while the remaining carbon atoms are disordered. Lowering the symmetry does not lead to a fully ordered structure. Additionally to this disorder there is a relatively high residual electron density, which could be interpreted as a second position of the whole structure (anion and cation) with an occupancy under 10%. Due to the poor quality of the data, a second crystal was measured, giving the same features. For the final refinement we used a merged data set of both crystals.

The disorder of the $[(i\text{-}Bu)_2AlF_2]^-$ anion in compound **1** can be understood by means of ab initio calculation, as a consequence of the floppy molecular backbone. The tendency for disorder is probed by the finding of computed imaginary or very low frequencies for two normal coordinates having the representations A_2 and B_1.[30] These modes are figuring the directions in which the disordering takes places. An equal superposition of $A_2 + B_1$ modes will result in a movement of only one alkyl group, while the other remains fixed. The finding that the experimental disorder is more pronounced at one alkyl group suggests that both of the instability coordinates are followed in the crystal structure.

In **3** two of the four $[AlF_4]^-$ ions are disordered. A second data collection was carried out, but did not show any improvement. The merged data set was used for the final refinement. The disordered parts in both structures were refined with distance restraints and restraints for the anisotropic displacement parameters. The nondisordered $[AlF_4]^-$ anions have Al−F bond lengths of 1.647 Å. A certain differentiation of the F−Al−F bond angles appears as a consequence of the environment. The crystal structure of **3** is quite similar (space group, unit cell parameters, disordering pattern) to a recently detected phase of $[Ph_4P][ClO_4]$.[31] The crystal analogy is understandable by comparing the symmetry and volume of the perchlorate and the tetrafluoroaluminate anion.

Table 1. Summary of X-ray Diffraction Data

	$[Me_4N][(i\text{-}Bu)_2AlF_2]$ (**1**)	$[Ph_4P][AlF_4]$ (**3**)
empirical formula	$C_{12}H_{30}AlF_2N$	$C_{24}H_{20}AlF_4P$
fw	253.35	442.35
cryst size (mm)	0.4 × 0.3 × 0.2/0.4 × 0.3 × 0.2	0.4 × 0.1 × 0.1/0.2 × 0.1 × 0.1
cryst syst	orthorhombic	tetragonal
space group	*Pnma*	$I\bar{4}$
a (Å)	19.208(4)	17.220(2)
b (Å)	8.783(2)	17.220(2)
c (Å)	9.720(2)	14.000(3)
cell vol V (Å^3)	1639.8(6)	4151(1)
Z	4	8
ρ_c (g mm^{-3})	1.026	1.416
μ (mm^{-1})	0.124	0.218
F(000)	560	1824
2θ range (deg)	4.7 to 55.3	3.3 to 55.3
data measd, unique	68853, 2033 [*R*(int) = 0.0364]	60925, 4819 [*R*(int) = 0.0525]
temp (K)	133(2)	133(2)
R,[a] wR_2[b] ($I > 2\sigma(I)$)	0.0696, 0.1816	0.0397, 0.0894
R, wR_2 (all data)	0.0744, 0.1860	0.0551, 0.0972
goodness of fit, *S*[c]	1.147	1.023
no. of refined params	109	331
no. of restraints	62	149
largest diff peak and hole (e Å^{-3})	+0.615/−0.388	+0.173/−0.285
absolute structure param		−0.02(9)

[a] $R = \sum||F_o| - |F_c||/\sum|F_o|$. [b] $wR_2 = [\sum w(F_o^2 - F_c^2)^2]/[\sum w(F_o^2)^2]^{1/2}$. [c] $S = [\sum w(F_o^2 - F_c^2)^2]/[\sum(n - p)]^{1/2}$.

Results and Discussion

The application of hydrogen difluoride for the preparation of new organometallic fluorides starting from metal alkyls stems from the fact that the moderately acidic proton of $[FHF]^-$ is able to eliminate an alkane from the metal-bonded alkyl groups, while the remaining empty coordination site can be occupied by a fluoride ion. The excess of $[FHF]^-$ leads to the formation of fluorides as the final and stable compounds (Scheme 1).

The $[FHF]^-$ anion is the most abundant species in the aqueous solution of HF, and obviously this is the effective agent when HF is used in fluorination reactions.[32] The ammonium salts $[R_4N][HF_2]$ are soluble in nonpolar solvents,[33−35] a feature that favors their use in organometallic chemistry.

Orbital Features of Organometallic and Inorganic Fluorides. A first insight into the electronic structure of organometallic fluorides is given with the help of molecular orbital

Scheme 1. Synthesis of Compounds **1**−**3**

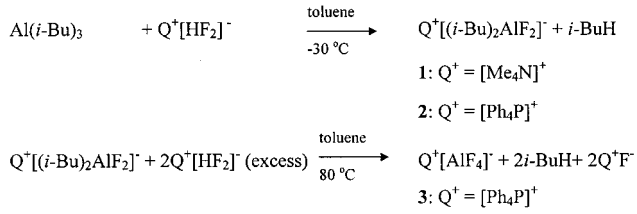

pictures, considering the Kohn−Sham functions from B3LYP calculations with the SV(P) basis set (Figure 3). We confine our report here only to a visual inspection of frontier orbitals. The $[AlF_4]^-$ anion shows the orbital pattern of a ligand-field regime, with the highest occupied orbitals preponderantly of ligand-type, while the empty frontier orbitals (a_1 and t_2) are originating from the s+3p valence shell of the Al(III) ion.

The organometallic fluorides $[Me_2AlF_2]^-$ and $[(i\text{-}Bu)_2AlF_2]^-$ show features similar to each other and qualitatively different from $[AlF_4]^-$. The highest two occupied MOs of the organometallic systems can be qualitatively regarded as a combination in-phase (a_1) and out-of-phase (b_2) of the hybrid orbitals located on the metal center and oriented toward the alkyl groups. These functions include combinations of s, p_z, and p_y orbitals of Al and AOs of the coordinated C atoms (Al−C bonds are located in the *yz* plane) and are the MOs with the maximal contribution to the Mulliken population on Al.

The search for the other two metal-type functions, spanning the a_1+b_1 representations (in order to complete a set assigned to a s+3p valence shell on Al), results in a corresponding pair among the empty orbitals, having shapes based on p_x and p_z central AOs. There exists a number of unoccupied orbitals, due to the nonbonding parts on the organic skeleton, intercalated between the a_1+b_2 (HOMO) and a_1+b_1 (post-LUMO) pairs. The shapes of the frontier orbitals suggest that the AlR_2^+ fragment has partial covalent character and forms ionic interactions with the two fluoride ions.

Hybrid-Orbital Model for the Stereochemistry of C_{2v}-Type Tetrahedral Units of Main Group Metals. A valuable simple perspective of the electronic structure of tetrahedral complexes of main group elements can be established using the hybridization language. The clue consists of the observation that for a series of previously reported $[Me_2MF_2]^-$ anions (M = Al, Ga, In)[36] all the experimental bond angles at the metal center can be fitted very well if they are defined as angles between the hybrid orbitals.

More specifically, under C_{2v} symmetry of the tetrahedral units, the hybrid orbitals in the (*xz*) plane can be written

$$|h_{1\pm}\rangle = \frac{1}{\sqrt{2}}(r|s\rangle + \sqrt{1-r^2}|p_z\rangle) \pm \frac{1}{\sqrt{2}}|p_x\rangle \qquad (1.a)$$

and regarded as oriented toward the fluorine atoms. The hybrids toward the alkyl groups in the (*yz*) plane are

$$|h_{2\pm}\rangle = \frac{1}{\sqrt{2}}(\sqrt{1-r^2}|s\rangle - r|p_z\rangle) \pm \frac{1}{\sqrt{2}}|p_y\rangle \qquad (1.b)$$

The angles between the components of $h_{1\pm}$ and $h_{2\pm}$ pairs and those between each h_1 component relative to each h_2, respectively, can be assimilated with the F−M−F, C−M−C, and

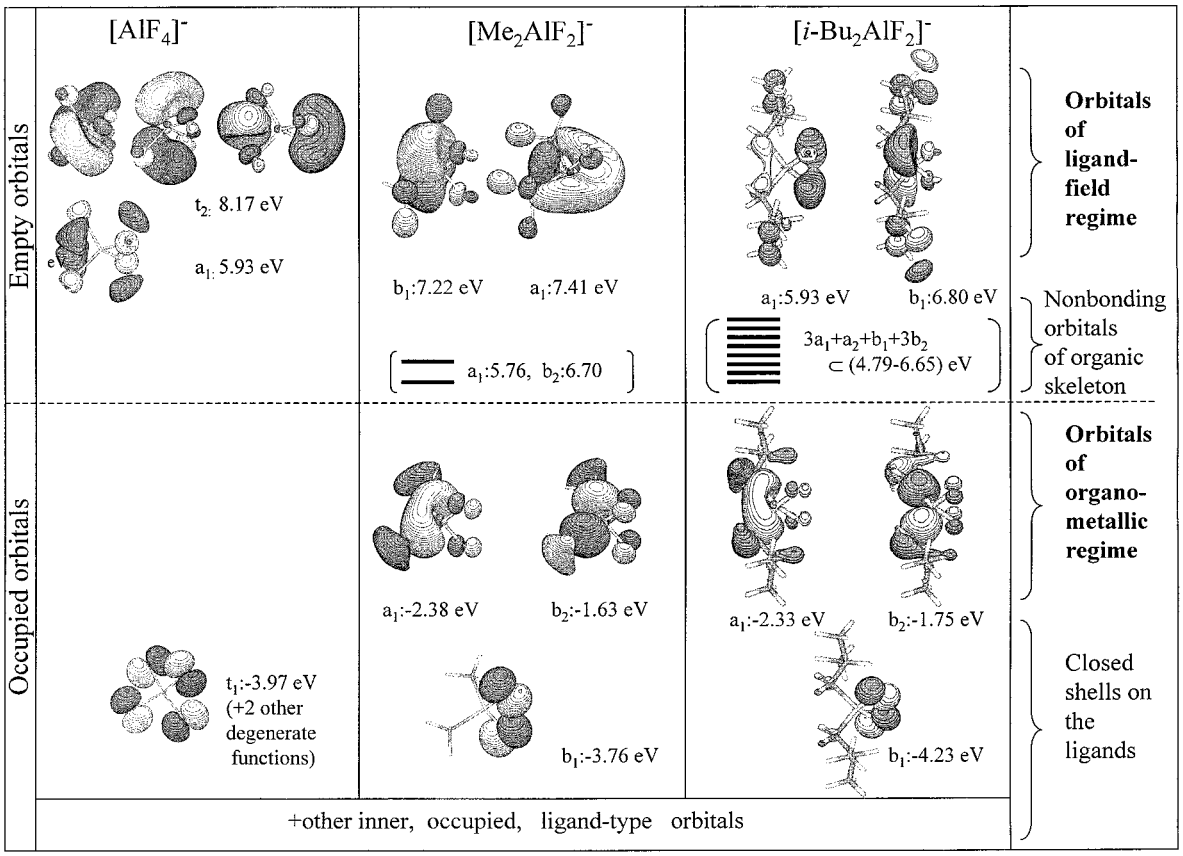

Figure 3. Kohn−Sham frontier orbitals in $[AlF_4]^-$, $[Me_2AlF_2]^-$, and $[(i\text{-}Bu)_2AlF_2]^-$ anions (from B3LYP calculations with SV(P) basis). The orbitals can be qualitatively regarded as having parentage in the s+3p valence shell of aluminum. This set has fully LUMO character in $[AlF_4]^-$ and is distributed between HOMO and post-LUMO in the organometallic ions.

Table 2. Experimental and Computed Geometry Parameters for $[R_2AlF_2]^-$ (R = *i*-Bu, Me)[a]

$[R_2AlF_2]^-$	Al−F (Å)	Al−C (Å)	F−Al−F (deg)	C−Al−C (deg)	*R* (deg)	*r*
R = *i*-Bu (**1**)						
experimental	1.711	1.99	101.6	111.5	3.29	0.6458
			105.28	114.29		
RHF,SV(P)	1.711	2.002	107.26	114.74	1.31	0.6544
			105.81	113.60		
RHF+MP2,SV(P)	1.725	1.993	107.77	118.19	3.05	0.6284
			104.24	115.71		
DFT(B-P),SV(P)	1.732	2.023	107.48	112.12	0.25	0.6759
			107.22	111.89		
DFT(B3LYP),SV(P)	1.721	2.016	107.45	112.48	0.40	0.6731
			107.03	112.11		
R = Me						
experimental	1.712	1.969	103.23	117.13	0.03	0.6110
			103.27	117.15		
RHF,SV(P)	1.710	2.007	107.23	112.32	0.20	0.6728
			107.01	112.13		
RHF+MP2,SV(P)	1.724	1.998	107.25	110.98	0.41	0.6826
			107.68	111.36		
DFT(B-P),SV(P)	1.733	2.023	107.23	110.85	0.48	0.6834
			107.74	111.30		
DFT(B3LYP),SV(P)	1.722	2.016	107.18	111.36	0.27	0.6795
			107.47	111.61		

[a] The second angles noted at each full line are results of the fit by the hybrid model. The last column gives the *r* hybridization parameter, and *R* measures the accuracy of the fit. $R = \sqrt{1/2((\alpha_{FMF}-\alpha_{FMF}^{hybrid})^2+(\alpha_{CMC}-\alpha_{CMC}^{hybrid})^2)}$. The angle C−M−F is, in C_{2v} symmetry, not independent and can be deduced from F−M−F and C−M−C ones, $\alpha_{CMF} = \arccos(-\sqrt{\cos(\alpha_{FMF})\cos(\alpha_{CMC})})$.

F−M−C parameters, having the following expressions:

$$(\text{F-M-F, C-M-C, F-M-C}) = \left(\arccos\left(-\frac{r^2}{2-r^2}\right), \arccos\left(-\frac{1-r^2}{1+r^2}\right), \arccos\left(-\frac{r\sqrt{1-r^2}}{\sqrt{(1+r^2)(2-r^2)}}\right)\right) \quad (2)$$

We observed the remarkable regularity that only one parameter (*r*) reproduces all coordination angles in the considered $[Me_2MF_2]^-$ anions with very good accuracy. This can be generalized to the useful working principle that all the mononuclear $[R_2MF_2]^-$ species of Al, Ga, and In are obeying this correlation (and possibly other MA_2B_2 systems,[37] except cases with very bulky and chelating ligands).

As a function of the mixing parameter *r* (extracted from geometry), the hybrids can be presented in the following form: $h_{1\pm} \equiv s^{2r2}p^{4-2r2}$, $h_{2\pm} \equiv s^{2-r2}p^{2+r2}$. When $r = 1/\sqrt{2}$, one obtains the equivalency of $h_{1\pm}$ and $h_{2\pm}$, at the sp^3 functions. For the actual convention of denoting the hybrids, the sum of their superscripts must give 4, that is, the number of handled orbitals. In other words, the average of $h_{1\pm}$ and $h_{2\pm}$ formally yields sp^3.

The hybrids revealed in the considered series are Al{$h_{1\pm} = s^{0.747}p^{3.253}$, $h_{2\pm} = s^{1.253}p^{2.747}$}, Ga{$h_{1\pm} = s^{0.538}p^{3.462}$, $h_{2\pm} = s^{1.462}p^{2.538}$}, and In{$h_{1\pm} = s^{0.392}p^{3.608}$, $h_{2\pm} = s^{1.608}p^{2.392}$}. The corresponding mixing parameter *r* can be found in the rows corresponding to the experimental entries in Tables 2 and 3. The fitted angles are presented below the experimental ones in the first entry of each compound in Tables 2 and 3.

Table 3. Experimental and Computed Geometry Parameters for $[Me_2MF_2]^-$ (M = Ga, In)[a]

$[Me_2MF_2]^-$	M−F (Å)	M−C (Å)	F−M−F (deg)	C−M−C (deg)	R (deg)	*r*
M = Ga						
experimental	1.839	1.969	98.74	125.10	0.15	0.5187
			98.94	125.17		
RHF,SV(P)	1.809	2.029	104.66	116.12	0.41	0.6274
			104.19	115.79		
RHF+MP2,SV(P)	1.817	2.023	104.75	114.97	0.01	0.6373
			104.76	114.98		
DFT(B-P),SV(P)	1.837	2.032	104.46	116.21	0.33	0.6255
			104.08	115.95		
DFT(B3LYP),SV(P)	1.827	2.029	104.59	116.50	0.52	0.6239
			103.98	116.08		
M = In						
experimental	2.043	2.150	95.68	132.09	0.41	0.4423
			96.22	132.28		
RHF,SV(P)	1.938	2.186	103.46	115.70	0.46	0.6241
			103.99	116.07		
RHF+MP2,SV(P)	1.957	2.193	103.32	115.37	0.67	0.6260
			104.10	115.91		
DFT(B-P),SV(P)	1.965	2.200	103.26	114.69	0.99	0.6310
			104.39	115.50		
DFT(B3LYP),SV(P)	1.953	2.189	103.42	114.85	0.82	0.6306
			104.37	115.53		

[a] The structure and notations are similar to those in Table 2.

One may note that the hybrids oriented toward the carbon atoms carry a more pronounced s character, at the expense of those oriented toward fluorine. The tendency can be qualitatively understood by the Bent rule.[38,39] According to this rule, the more pronounced s character of the hybrids is concentrated on the side of the electropositive ligands, while the electronegative ones remain as hybrids with a higher p contribution. This is a first explanation for the experimentally observed tendency that the F−M−F angle is decreasing while the C−M−C angle is increasing in the order of Al, Ga, In. Indeed, with the progressive lowering of the s-part, the hybrid angle varies in the direction of the 90° limit, as is seen from the experimental data in Tables 2 and 3, and this is also revealed in the given composition of $h_{1\pm}$ hybrids.

A general validity of the hybridization pattern of bond angles may be applied for the $[(i\text{-Bu})_2AlF_2]^-$ anion as a rough approximation of the geometry (static limit) using the angles available from the disordered structure. In this context the $[(i\text{-Bu})_2AlF_2]^-$ and $[Me_2AlF_2]^-$ species should be qualitatively similar, as is also probed by the calculated results (Table 2).

The results of geometry optimization for the $[Me_2MF_2]^-$ complexes (M = Al, Ga, In) follow the tendency of experimental bond lengths and angles (Tables 2 and 3). However, the bond angle variation is better accounted in the Al, Ga sequence than in the Ga, In congeners. The anions were computed in a vacuum, and the results were not improved after including the Madelung field as point charges from a few surrounding cells. Furthermore, the considered units were taken from isomorphous crystals ($[Bu_4N][Me_2MF_2]$) with highly similar cell parameters and intermolecular distances. Therefore, the Madelung field is similar in all the complexes and plays no decisive role in establishing the tendency of bond angle variation. As the calculations for the free anions show, this is an intrinsic feature of the complexes themselves.

Hybrid-Type Angles as Experimental Criterion for Consideration of ab Initio Calculations. Hybrid patterns of bond

(37) Atwood, D. A. *Coord. Chem. Rev.* **1998**, *176*, 407−430.

(38) Bent, H. A. *Chem. Rev.* **1961**, *61*, 275−311.

(39) Fröhlich, N.; Frenking, G. In *Solid State Organometallic Chemistry: Methods and Applications;* Gielen, M., Willem R., Wrackmeyer, B., Eds.; John Wiley & Sons: New York, 1999; pp 173−226.

angles are remarkably adequate as real geometry; therefore the capacity of electronic structure calculations to reproduce this regularity will be proposed as a key to judge the results of ab initio calculations.[40] A first measure is given by the value of the fitted mixing parameter (*r*) in comparison with the experimental data (Tables 2 and 3). All the methods have the tendency to overestimate the value of *r*, especially with an increased deviation for the heavy metals. The accurate description of heavy elements on one side and of the anionic molecules on the other is a notoriously difficult task, and the observed hybrid-type regularities can be taken as a new, chemically meaningful, test of the method.

Another measure of the ab initio results can be considered in the quality of a hybrid fit with respect to the computed angles, presented as mean square deviation in column *R* of Tables 2 and 3. This criterion is practically not related to the capability of the method in reproducing the experimental bond angles. Each calculation contains small deviations from the hybrid angle pattern. Moreover, we checked a few other basis sets (ranging from sto3g to cc-pvtz) and noted a similar decline.

The present analysis demonstrates that the hybridization is a valuable tool even in the age of advanced computer application in quantum chemistry.[41,42] According to the natural bond orbital concepts,[43] the hybrids are appropriate objects for accounting for the so-called localized character of the correlation effects.[44]

The relatively large radius of the central atom and the small radius of the bonded ones make the validity of the hybridization scheme in the $[Me_2MF_2]^-$ complexes (M = Al, Ga, In) free from strains due to sterical hindrance. A short comparison of the goodness of fit (with formula from Table 2) for other systems, like SiH_2F_2 ($R = 0.44$), CH_2F_2 ($R = 0.97$), and CH_2Cl_2 ($R = 2.28$), shows that light central atoms and heavy ligands enforce a deviation of the geometry from the hybrid pattern. The broad investigation of MA_2B_2-type molecules by the given model is left as a matter of other studies. The role of d orbitals in the generalized hybridization schemes and in connection with the practical basis sets of electron structure calculation remains also a subject of further investigation.

Mutual Influence of Hard and Soft Ligands in Organometallic Fluorides. Compounds **1** and **2** on one side and **3** on the other (according to HSAB predictions) show certain mutual differences in the electronic structure. This problem will be addressed using the DFT calculations with ADF code[45] as a versatile tool for obtaining absolute values[46] for electronegativities and hardness.[47]

For the neutral ligands the following ligand electronegativities are estimated: χ_F 11.93, χ_{Me} 5.45, and χ_{i-Bu} 4.29 eV. The hardness parameters are a measure of Lewis basicity of the ligands (η_F 8.10, η_{Me} 4.79, η_{i-Bu} 3.82 eV).[48] Obviously, the fluorine is revealed as the most electronegative and hardest in this series. For the isobutyl group the lower electronegativity and hardness can be related with an inductive effect.

The neutral aluminum has the estimated parameters χ_{Al} 4.64 eV and η_{Al} 2.98 eV, while the organometallic fragment taken as the neutral $AlMe_2$ species has the values χ_{AlMe2} 2.77 eV, η_{AlMe2} 2.62 eV. The latter is less hard (weaker acid) compared to the aluminum atom. At the same time the lower electronegativity suggests that $AlMe_2$ is more electropositive compared to Al. This will result in a higher electronegativity difference of $AlMe_2$ than that of Al with respect to fluorine. Therefore the Al−F bonds are predicted to be more ionic in organometallic fluorides than in the homoleptic inorganic fluorides.

However, a certain underestimation appears in the calculated hardness of aluminum. The apparent failure of calculation to detect more clearly the expected HSAB affinity between aluminum and fluoride is probably a matter of not including in the calculation the effects of interatomic interactions between the acidic and basic partners. A future task of theoretical work devoted to HSAB principle is to design a method to be able to provide electronegativity and hardness corresponding to atoms in molecules. In fact, one may suggest that HSAB is better kept in terms of electronegativity and hardness calculated for atoms in molecules than using quantities estimated for isolated atoms. Despite the huge literature devoted to the formalism and computation of electronegativity and hardness in relation to DFT schemes, the systematization of the structural chemistry in terms of a quantitative HSAB frame is still incomplete. A partial improvement is given here, using the concept of the mutual influence of ligands.

An important result of the actual analysis was the detection of a mutual influence of the hard and soft ligands, revealed on the $[Me_2AlF_2]^-$ study case. A comparison of this anion with the $[AlF_4]^-$ and $[AlMe_4]^-$ ones was carried out by means of DFT calculations, considering the ionic vs covalent bonding in the Al−F and Al−Me bonds. For this purpose we applied the so-called transition-state method by Ziegler et al.[49] as implemented in ADF code.[45] Using optimized geometries (T_d for $[AlF_4]^-$ and $[AlMe_4]^-$ and C_{2v} for $[Me_2AlF_2]^-$), we calculated

(40) This series of calculations was made with the GAMESS package: Schmidt, M. W.; Baldridge, K. K.; Boatz, J. A.; Elbert, S. T.; Gordon, M. S.; Jensen, J. H.; Koseki, S.; Matsunaga, N.; Nguyen, K. A.; Su, S. J.; Windus, T. L. *J. Comput. Chem.* **1993**, *14*, 1347−1363. The DFT optimizations were repeated in TURBOMOLE: Ahlrichs, R.; Bär, M.; Häser, M.; Horn, H.; Kölmel C. *Chem. Phys. Lett.* **1989**, *162*, 165.

(41) (a) Root, D. M.; Landis, C. R.; Cleveland, T. *J. Am. Chem. Soc.* **1993**, *115*, 4201−4209. (b) Landis, C. R.; Cleveland, T.; Firman, T. K. *J. Am. Chem. Soc.* **1995**, *117*, 1959−1860. (c) Barbier, C.; Berthier, G. *Adv. Quantum Chem.* **2000**, *36*, 1−24.

(42) (a) Nicolaides, C. A.; Komninos, Y. *Int. J. Quantum Chem.* **1998**, *67*, 321−328. (b) Komninos, Y.; Nicolaides, C. A. *Int. J. Quantum Chem.* **1999**, *71*, 25−34.

(43) Reed, A. E.; Curtiss, L. A.; Weinhold, F. *Chem. Rev.* **1988**, *88*, 899−926.

(44) (a) Saebo, S.; Pulay, P. *Annu. Rev. Phys. Chem.* **1993**, *44*, 213−236. (b) Schutz, M.; Hetzer, G.; Werner, H. J. *J. Chem. Phys.* **1999**, *111*, 5691−5705.

(45) (a) Amsterdam Density Functional (ADF) package: te Velde, G.; Baerends, E. J. *J. Comput. Phys.* **1992**, *99*, 84−98. (b) In present calculations we employed the implemented basis sets of triple-ζ type and the PW91 density functional set.

(46) The chemical hardness was computed from numerical derivatives of total energies, $\eta = 1/2\partial^2E/\partial n^2$, obtained after slight variations of the corresponding total charge and populations. The systems were taken in spin nonpolarized averaged states. The variation of charge was distributed over the frontier orbitals in such a way that allows the assignment related to hybrid orbitals. For instance, for aluminum, the $s^{0.75\pm x}$, $p^{2.25-3x}$, small variations simulate an sp^3 state of the atom. For the neutral $AlMe_2$ fragment, the direct calculation yields a singly occupied a_1 HOMO orbital and a b_1 LUMO, which can represent the pair of hybrids able to bind the fluorine. Therefore, we considered the smearing-out of the electrons over these functions into $a_1^{0.5\pm x}b_1^{0.5\pm x}$ configuration.

(47) Parr, R. G.; Yang, W. *Density Functional Theory in Atoms and Molecules;* Oxford University Press: NewYork, 1989.

(48) For the neutral fluorine and alkyls, the computed electronegativity and hardness were based on the variation in the population of the HOMO orbital, with $0.5 \pm x$ for both α and β fractions of the spin nonpolarized DFT calculation.

(49) (a) Ziegler, T.; Rauk, A. *Theor. Chim. Acta* **1977**, *46*, 1−10. (b) Ziegler, T.; Rauk, A. *Inorg. Chem.* **1979**, *18*, 1558−1565. (c) Ziegler, T.; Rauk, A. *Inorg. Chem.* **1979**, *18*, 1755−1759.

Table 4. Partition of the Total Energy ($E_t = E_P + E_{el} + E_{orb}$) of Bond Formation, as Results from the Transition State Method[a]

bond formation	E_t	E_P	E_{el}	E_{orb}
$AlF_3 + F^- \rightarrow AlF_4^-$	−6.17	3.57	−7.44	−2.31
$AlMe_3 + Me^- \rightarrow AlMe_4^-$	−4.45	5.50	−7.01	−2.93
$AlF_2Me + Me^- \rightarrow AlF_2Me_2^-$	−5.26	5.77	−8.03	−3.00
$AlFMe_2 + F^- \rightarrow AlF_2Me_2^-$	−4.93	4.07	−6.31	−2.69

[a] See the text for definition of column entries. All quantities are in eV.

the total energy of interaction (E_t) between the corresponding fragments (Table 4).

The result that the Al−F in $[AlF_4]^-$ is stronger than the Al−Me bond in $[AlMe_4]^-$ (comparing E_t in Table 4) is in line with the HSAB concept. The covalency of the Al−Me bonds (measured by E_{orb}) is invariably higher compared to the Al−F. Consequently the reciprocal affinity between aluminum and fluorine seems to have a noticeable ionic character.

Examining the charges from Mulliken population analysis, one may consider $[AlF_4]^-$ definitely more ionic (q_{Al} 2.116, q_F −0.779) than $[AlMe_4]^-$ (q_{Al} 1.282, q_{Me} −0.571). Moreover, in $[Me_2AlF_2]^-$ the fluorine is more ionic (q_F −0.805) than in the tetrafluoroaluminate.

A drastic change of bonding energies appears in $[Me_2AlF_2]^-$, where Al−F becomes weaker than Al−Me. The weakening of the Al−F bond in the organometallic structures (compared to the inorganic anion) is clearly seen in the experimental Al−F bond lengths ($[Me_2AlF_2]^-$, $[(i\text{-}Bu)_2AlF_2]^-$ ∼1.71 Å, $[AlF_4]^-$ ∼1.65 Å).

Thus, a distinguished reciprocal influence of ligands occurs in the mixed ligand complex. Namely, the former stronger bonding partner strengthens the initially weaker one, while the latter exerts an opposite influence on the first. This phenomenon can be understood in such a way that the mixed hardness allows the polarization of the central ion. This corresponds to the mixing of odd and even atomic orbitals, which is symmetry forbidden in tetrahedral moieties ($[AlMe_4]^-$ and $[AlF_4]^-$). The observations from the previous section show that the polarization effects can be surprisingly accurate confined to the model of hybridized s and p orbitals. The polarization allows the deformation of the aluminum center in two halves differentiated by the HSAB factors. One face, toward the alkyl groups, behaves as a weak acid, while the other, toward the fluorine ligands, appears as a hard acid. At the same time, the lower hardness corresponds to more diffuse AOs, allowing a better overlapping in the Al−C bonds.

Other useful insights into the bonding situation are gained by the dichotomy of the total energy, when the repulsive Pauli exchange (E_P), cohesive electrostatic energy (E_{el}), and the orbital term (E_{orb}) are considered as components.[52] Examining the E_P term (both in absolute value and relative to E_t), the most significant repulsion effects are encountered for the alkyl group.

The E_P (quantum repulsion of closed shells) and the E_{el} (classical electrostatic interactions) terms are quantities revealed when the formation of the bonding between the fragments is prevented by enforced restriction of the orbital mixing between the wave functions located on the defined subsystems. The relaxation from hypothetical fragments to the final bond is possible after the allowance of orbital mixing (E_{orb} stabilization).

The sum $E_P + E_{el}$ (the so-called steric term) shows the interesting feature of comparable values for Al−F and Al−Me bonds. This suggests that the optimum geometry can be interpreted as a balance of interligand repulsion. The high repulsion terms found in Al−Me bonds shows that the centroids of the negative charges (which originate from the lone pairs of the methyl groups directed to aluminum) are located close to each other. This results in the strong repulsion between electron densities of different Al−C bonds.

On the contrary, in bonded fluoride, due to its intrinsic hardness, the negative charge is less deformed compared to the spherical anion, yielding a more relaxed repulsion between ligands. The tendency for a bigger C−Al−C angle compared to the F−Al−F one can be understood as driven by the higher content of repulsion terms in Al−C bonds.

Phenomenological Model for the Energy of a Hybridized Atom (Equating the Bent Rules). Previously it was shown that the variation of bond angles in the $[R_2MF_2]^-$ series is in line with the Bent rules. The energy factors determining the preference of electronegative ligands for almost unhybridized orbitals are qualitatively related to the easier ionization of the metal when electrons are taken from its p orbitals. We target here a simple function able to model this factor, starting from the data offered by appropriate quantum evaluation of the energies of various atomic states. The energy ($W_M(n_1,n_2)[r]$) of the atom in a general $(h_{1+})^{n_1}(h_{1-})^{n_1}(h_{2+})^{n_2}(h_{2-})^{n_2}$ configuration was conceived as a continuous function of hybrid populations (n_1 and n_2) and mixing parameter, r. The continuity of the function ensures the availability of orbital electronegativities (χ) and hardness (η), as derivatives of the total electronic energy,[46] with respect to the electron number.

According to Gyftopoulos theorem,[51] a system with fractionally occupied states can be conceived as a result of weighted superposition of the energies for various integer-populated configurations. Therefore the W_M energy for a general population at the hybrids can be obtained through an adequate interpolation over energies of certain reference configurations. They are available at integer values of the hybrid occupation numbers. The energies of integer-populated configurations can be correspondingly converted from hybrids to occupations of s and p shells, which can be computed from the configuration interaction on the Al atom. The details of construction are shown in the Appendix.

The W_M function allows (as a heuristic model) the estimation of hybridization degrees, which yield the minimum energy for a complete area of varying the hybrid orbital populations. Thus, the energy of the central atom-in-molecule is proposed as the phenomenological key for the mutual relationship of hybridization degree versus population balance. The surface from Figure 4 contains such dependence for the population (range $n_1 \subset (0, 2)$, $n_2 \subset (0, 2)$, restricted with $n_1 + n_2 < 4$).

Figure 4 shows that the hybridization degree decreases to a small value (e.g., 0.2) when the population balance is $n_1 < n_2$ and approaches the plateau of $r = 1$ when $n_1 > n_2$. Fixing the subscript 1 for fluorine and 2 for alkyl ($[R_2AlF_2]^-$), it is possible to see that the case $n_1 < n_2$ corresponds to the ionic nature of the hybrids oriented toward the fluorine face. Such a situation results naturally as a consequence of the electronegativity equalization principle.[52] According to equation 2, this corresponds to smaller angles for the moiety containing electronegative ligands. The map from Figure 4 offers a semiquantitative modeling of the empirical Bent rules.

(50) Diefenbach, A.; Bickelhaupt, F. M.; Frenking, G. *J. Am. Chem. Soc.* **2000**, *122*, 6449−6458.
(51) (a) Gyftopoulos, E. P.; Hastopoulos, G. N. *Proc. Natl. Acad. Sci. U.S.A.* **1965**, *60*, 786−793. (b) Perdew, J. P.; Parr, R. G.; Levy, M.; Balduz, J. L., Jr. *Phys. Rev. Lett.* **1982**, *49*, 1691−1694. (c) Zhang, Y.; Yang, W. *Theor. Chem. Acc.* **1999**, *103*, 346−348.
(52) Sanderson, R. T. *Science* **1951**, *114*, 670−672.

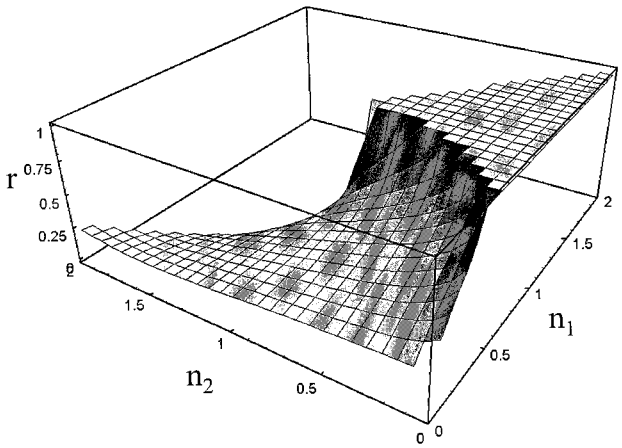

Figure 4. Hybridization degree (r), giving the minimum energy of the central atom as a function of the populations n_1 and n_2, describing a general valence state of C_{2v} symmetry. The surface is generated with the W_M function constructed for aluminum, but the pattern is general for main group metals.

The given model is qualitatively valid for explaining the angular tendencies in a general $[MA_2B_2]$ complex (M = Al, Ga, In, or even throughout all main group metal elements). The reason for expected generality is that the relative ordering of the averaged energies of the spectral terms (which determine the pattern of W_M) is similar for the different main group atoms (e.g., $E(s^2p^{n-2}) < E(sp^{n-1}) < E(p^n)$, simply due to the s < p orbital energy ordering).

The bond angle variation in the $[Me_2MF_2]^-$ series can be explained by accepting that the electronegativity is in the order Al > Ga > In. The real order can be a matter of dispute and further investigation (different sources indicating different values[53,54]). However, the actual modeling is consistent with the Al > Ga > In order and therefore appears to be effectively valid. Thus, the electronegativity difference between the central atom and fluorine will increase in the same order. This results in the enhanced M→F charge transfer, which leads to a smaller n_1-population in the orbitals oriented toward fluorine. The Al, Ga, In series is arranged in the order of the more pronounced $n_1 < n_2$ tendency. Figuring this order on the given surface (Figure 4), it is seen that it corresponds to the decreasing hybridization parameter r. The more pronounced $n_1 < n_2$ separation from Al to In is revealed also by the population analysis in the ab initio calculations.

The qualitative utility of the above model can be extended further. One may predict, for example, the geometry changes when $[R_2AlF_2]^-$ appears as a bridge in polynuclear systems. Examples of this type are $[Cp_2Ti(\mu\text{-}F)_2AlEt_2]_2$,[55] *cis*-$\{[Cp^*ZrMe(\mu\text{-}F)][(\mu\text{-}F)_2AlMe_2]\}_2$,[56] and *cis*-$\{[Cp^*HfMe(\mu\text{-}F)][(\mu\text{-}F)_2AlMe_2]\}_2$.[57] The formation of a bridge reduces the negative charge on fluorine, but enhances its electronegativity.[58] Therefore, a bridged $[Me_2AlF_2]^-$ moiety will have a more pronounced $n_1 < n_2$ balance compared to the free one. This corresponds to moving to lower values of r on the surface (Figure 4), which is correlated to smaller F−Al−F angles. Indeed, in the compounds $[Cp_2Ti(\mu\text{-}F)_2AlEt_2]_2$, *cis*-$\{[Cp^*ZrMe(\mu\text{-}F)][(\mu\text{-}F)_2AlMe_2]\}_2$, and *cis*-$\{[Cp^*HfMe(\mu\text{-}F)][(\mu\text{-}F)_2AlMe_2]\}_2$, the F−Al−F angles are (100.18°, 96.85°, and 96.10°) smaller than that of the free $[Me_2AlF_2]^-$ (Table 2). The dependence of the F−Al−F angle on the nature of the transition metal bonded to fluorine can be understood by considering the degree of the covalency increasing from Ti to Hf. The fluorine will be more neutral due to forming the bond with the heavier transition atom and therefore more electronegative.

Another compound containing the $[R_2MF_2]^-$ anion is Cs-$[Me_2GaF_2]$,[59] with a polymeric structure, where each fluorine atom has close contacts with two cesium atoms. In this compound the F−Ga−F angle is slightly smaller (96.7(3)°), while the C−Ga−C angle is increased (127.8(6)°), compared with $[Me_2GaF_2]^-$ (Table 3). This can be interpreted by a decrease of the hybridization parameter to $r = 0.46$ for the unit embedded in the polymeric structure. The effect can be assigned to the polarization exerted from cesium to fluorine, thus causing further Ga→F charge transfer (lowering of n_1).

A similar bridge is found in $[Cs(THF)_{0.5}(Me_2GaF_2)]$,[60] where the bond angles are closer to the free moiety (F−Ga−F 97.1(2)°) and C−Ga−C 129.8(4)°). Here the Cs atoms are complexed with THF and exert a smaller perturbation to the adjacent fluorine atoms.

A qualitatively different situation is encountered in Cs-$[(PhCH_2)_2GaF_2]$,[61] which shows an extended structure with Cs−F−Ga bridges. Here, the F−Ga−F and C−Ga−C angles cannot be fitted with a unique parameter r. The deviation is caused by the strain of packing forces, the crystal structure revealing an η^6-like interaction between phenyl groups and cesium atoms.

In summary, the designed W_M function of the central atom allowed the establishment of a connection between the differentiated orbital hybridization and the electron populations on the metal complexes. The model can be used to rationalize the stereochemistry, assuming that the dependence on hybridization effects on the central atom is the leading term in molecular energy.[42] According to preliminary verifications, the model works for various MA_2B_2 systems (M = C, Si, Ge, Sn; A,B = R, F, Cl) where the π bonding and d orbitals are supposed to play no significant role. The ionic nature and weak covalency of the analyzed $[R_2MF_2]^-$ systems satisfy with particular accuracy the outlined premises. The present model should not be used for molecules such as SO_2Cl_2 or $TiMe_2Cl_2$, although further similar modeling is in principle possible.

Conclusions

The synthesis of organometallic fluorides is one of the challenging topics of modern chemistry, while it can be conceived as working against the HSAB rules of affinity. The use of $[FHF]^-$ as a reagent provides the interplay of chemical rules that govern the protonic definition and reactivity of acids and bases. The use of $[FHF]^-$ can be emphasized as a general route to the systematic synthesis of organometallic fluorides.

(53) (a) Robles, J.; Bartolotti, L. J. *J. Am. Chem. Soc.* **1984**, *106*, 3723−3727. (b) Bartolotti, L. J. *Struct. Bond.* **1987**, *66*, 27−40. (c) Pearson, R. G. *Inorg. Chem.* **1988**, *27*, 734−740.
(54) (a) Böhm, M. C.; Schmidt P. C. *Ber. Bunsen-Ges. Phys. Chem.* **1986**, *90*, 913−919. (b) Sen, K. D.; Böhm, M. C.; Schmidt, P. C. *Struct. Bond.* **1987**, *66*, 99−123.
(55) Yu, P.; Montero, M. L.; Barnes, C. E.; Roesky, H. W.; Usón, I. *Inorg. Chem.* **1998**, *37*, 2595−2597.
(56) Herzog, A.; Roesky, H. W.; Zak, Z.; Noltemeyer, M. *Angew. Chem., Int. Ed. Engl.* **1994**, *33*, 964−966; *Angew. Chem.* **1994**, *106*, 1035−1037.
(57) Herzog, A.; Roesky, H. W.; Jäger, F.; Steiner, A.; Noltemeyer, M. *Organometallics* **1996**, *15*, 909−917.
(58) This is a general tendency in the electronegativity (χ) vs charge (q) dependence and is related with the positive hardness, $\eta = d\chi/dq$.
(59) Kopp, M. R.; Neumüller, B. *Z. Anorg. Allg. Chem.* **1998**, *624*, 1393−1394.
(60) Kopp, M. R.; Kräuter, T.; Werner, B.; Neumüller, B. *Z. Anorg. Allg. Chem.* **1998**, *624*, 881−886.
(61) Neumüller, B.; Gahlman, F. *Chem. Ber.* **1993**, *126*, 1579−1585.

The actual approach targeted the fluorinated compounds of aluminum and brought into discussion the detailed aspects that relate the electronic structure with the HSAB concept. The given analysis elaborated a phenomenological model able to rationalize the factors determining the bond angle in $[R_2MF_2]^-$, which offers a more quantitative basis to the Bent rules. The model assumes a hybridization-driven bond-angle pattern and constructs the energy of the central atom as a function of hybrid populations. The condition of minimum energy gives a map of preferred hybridization degree, as a function of orbital population balance. This can be used as a tool to understand the bond angle variation in the stereochemistry of various members of $[R_2MF_2]^-$ complexes (free or bridged units). The systematic HSAB approach for structural problems, by means of electronic structure calculations and phenomenological models, opens new views on the principle and methods of chemical synthesis.

Acknowledgment. M.F. is grateful to the Alexander von Humboldt Foundation for the research fellowship. The financial support of the Deutsche Forschungsgemeinschaft is acknowledged. We are very thankful to one of the referees for his valuable comments.

Appendix

The key for obtaining the energy of the central atom, $W_M(n_1,n_2)[r]$, as a continuous function of hybrid populations, n_1, n_2, and hybridization degree, r, is to consider it as a weighted superposition of energies taken at all possible integer-populated configurations denoted w_{ij}.

$$W_M(n_1,n_2)[r] = \sum_{i,j} c_{ij}(n_1,n_2) w_{ij}(r) \qquad (A.1)$$

The i and j indices are paralleling the couples of integer occupation numbers possible for h_1 and h_2 hybrids, respectively. The defining condition is that the weighting coefficients should recover the energy of reference configurations when n_1 and n_2 are taken as corresponding integers (i, j = 0, 1, or 2):

$$W_M(i,j)[r] = w_{ij}(r) \equiv c_{ij}(k,l) = \delta_{ik}\delta_{jl} \qquad (A.2)$$

The (k,l) pairs are running over the same set of values as the (i,j) ones.

The general relations between population on hybrids versus s and p shells are

$$n_s = n_1 r^2 + n_2(1 - r^2);\ n_z = n_1(1 - r^2) + n_2 r^2;\ n_x = n_1,\ n_y = n_2 \qquad (A.3)$$

The form of $w_{ij}(r)$ can be taken as quadratic interpolation over the distinguished values given below:

$$w_{ij}(r=1) = w_{ji}(r=0) = w(s^i p_z^j p_x^i p_y^j),\ w_{ij}(r=0) = w_{ji}(r=1) = w(s^j p_z^i p_x^i p_y^j),\ w_{ij}(r=1/\sqrt{2}) = w_{ji}(r=1/\sqrt{2}) = w(s^{i+j/2} p_z^{i+j/2} p_x^i p_y^j) \qquad (A.4)$$

Example: $w_{20}(r=1) = w(s^2p_z^2)$, $w_{20}(r=0) = w(p_z^2p_x^2)$, and $w_{20}(r=1/\sqrt{2}) = w(s^1p_z^1p_x^2)$.

The energies of various orbital configurations over s and p valence shells are obtained by selecting corresponding diagonal matrix elements from the output of the configuration interaction calculations of the central atom with various charges (we used for this purpose a pVTZ basis set for aluminum). The elements with the same orbital population but different spin coupling were averaged, to get the spin unpolarized meaning, as is appropriate for the diamagnetic compounds $w(s^1p_z^1p_x^2) = (w(s(\alpha)p_z(\alpha)p_x^2) + w(s(\alpha)p_z(\beta)p_x^2))/2$. The orbital basis for estimating such matrix elements was prepared under the generalized valence bond (GVB) method, where in the case of degenerate ground terms the coupling elements of the Fock matrix were imposed in a way that corresponds to the spherically averaged ground states.

Apparently a problem arises when $(i + j)/2$ is a half-integer. This case can be empirically solved taking an interpolation on integer populations with $(i + j \pm 1)/2$, $(i + j \pm 3)/2$. Aside from the handling of matrix elements from configuration interactions (computed with GAMESS) the w_{ij} energies can be directly computed imposing the given orbital occupancies in ADF code. Both versions give a similar pattern of the final W_M energy function. To establish different populations at s, p_x, p_y, and p_z orbitals, the calculation of the atom under D_2 symmetry is a convenient procedure.

The coefficients $c_{ij}(n_1,n_2)$ from eq A.1 can be proposed in a polynomial form where, for each of them, the powers k and l in the $n_1^k n_2^l$ monomial terms are running with the same values as for the (i,j) couples of indices denominating the available integer occupation numbers:

$$c_{ij}(n_1,n_2) = \sum_{k,l} A_{ij}^{kl} n_1^k n_2^l \qquad (A.5)$$

The condition of eq A.2 results in the full determination of the A_{ij}^{kl} elements from various sets of linear equations (one equation system per ij couple):

$$\sum_{k,l} A_{ij}^{kl} i^k j^l = \delta_{ik}\delta_{jl} \qquad (A.6)$$

The solving of eq A.6 (for the cases running with i, j, k, l = 0, 1, 2) leads to the finding of coefficients (eq A.5) (then, replaced in eq A.1):

$$W_M(n_1,n_2)[r] = \frac{1}{4}(n_1-2)(n_1-1)(n_2-2)(n_2-1)w_{00}(r) + \frac{1}{2}(n_1-2)(n_1+1)(n_2-2)n_2 w_{01}(r) + \frac{1}{4}(n_1-2)(n_1-1)(n_2-1)n_2 w_{02}(r) + \frac{1}{2}(n_1-2)n_1(n_2-2)(n_2-1)w_{10}(r) + (n_1-2)n_1(n_2-2)n_2 w_{11}(r) + \frac{1}{2}(n_1-2)n_1(n_2-1)n_2 w_{12}(r) + \frac{1}{4}(n_1-1)n_1(n_2-2)(n_2-1)w_{20}(r) + \frac{1}{2}(n_1-1)n_1(n_2-2)n_2 w_{21}(r) + \frac{1}{4}(n_1-1)n_1(n_2-1)n_2 w_{22}(r) \qquad (A.7)$$

The above formula is continuous and differentiable in all the parameters, n_1, n_2, and r, and combines the valence bond and DFT-like approach in the model based on the hybridization concept.

Supporting Information Available: Tables listing detailed crystallographic data, atomic positional parameters, and bond lengths and angles. This material is available free of charge via the Internet at http://pubs.acs.org.

IC010131G